

THE PROCESS

$e^+e^- \rightarrow \omega\pi^0 \rightarrow \pi^0\pi^0\gamma$ UP TO 1.4 GEV.

M.N.Achasov, K.I.Beloborodov, A.V.Berdyugin,
 A.G.Bogdanchikov, A.V.Bozhenok, D.A.Bukin, S.V.Burdin,
 V.B.Golubev, T.V.Dimova, A.A.Drozdetsky, V.P.Druzhinin*,
 M.S.Dubrovin, V.N.Ivanchenko, A.A.Korol, S.V.Koshuba,
 G.A.Kukartsev, I.N.Nesterenko, E.V.Pakhtusova, E.A.Perevedentsev,
 V.M.Popov, A.A.Salnikov, S.I.Serednyakov, V.V.Shary, Yu.M.Shatunov,
 V.A.Sidorov, Z.K.Silagadze, A.N.Skrinsky, A.G.Skripkin,
 Yu.V.Usov, A.A.Valishev, A.V.Vasiljev, Yu.S.Velikzhanin

Budker Institute of Nuclear Physics, 630 090, Novosibirsk, Russia

Abstract

The cross section of the $e^+e^- \rightarrow \omega\pi^0 \rightarrow \pi^0\pi^0\gamma$ reaction was measured by the SND detector at VEPP-2M e^+e^- collider in the energy range from threshold up to 1.4 GeV. Results of the cross section fitting by the sum of ρ , ρ' and ρ'' contributions are presented.

1 Introduction

The process of e^+e^- annihilation into hadrons in the 1–2 GeV energy region is an important source of information about excited states of light vector mesons ρ , ω and ϕ . Parameters of these states are still not well established mainly due to poor accuracy of existing experimental data. Recently new data in this energy region became available. The cross sections of the reactions $e^+e^- \rightarrow 3\pi$ [1] and $e^+e^- \rightarrow 4\pi$ [2] were measured at VEPP-2M

*e-mail: druzhinin@inp.nsk.su

collider. Accuracy was also significantly improved in the recent measurements of $\tau \rightarrow 2\pi\nu_\tau$ and $\tau \rightarrow 4\pi\nu_\tau$ spectral functions [3, 4, 5] related to corresponding e^+e^- annihilation cross sections by the CVC hypothesis [14].

The reaction $e^+e^- \rightarrow \omega\pi^0$ is one of the dominant processes in the energy range from 1 to 2 GeV. The PDG values for the mass and width of the $\rho'(1450)$ meson [7] are based mainly on phenomenological studies of this process [6]. The most precise measurements of the $e^+e^- \rightarrow \omega\pi^0$ cross section and $\tau \rightarrow \omega\pi\nu_\tau$ spectral function were done in [2, 8, 4]. All these experiments addressed the 4π final state into which other intermediate states, for example $a_1\pi$, contribute significantly. In this work the $e^+e^- \rightarrow \omega\pi^0$ reaction was studied in the $\pi^0\pi^0\gamma$ final state where other contributions are much smaller. This allows to avoid systematic errors inherent to the $e^+e^- \rightarrow 4\pi$ channel due to non-trivial background subtraction, which must take into account interference effects. The process $e^+e^- \rightarrow \omega\pi^0 \rightarrow \pi^0\pi^0\gamma$ was studied for the first time in [9] where 20% statistical accuracy was achieved.

2 Detector and experiment

SND is a general purpose non-magnetic detector [10]. Its main part is a three-layer scintillation electromagnetic calorimeter consisted of 1630 NaI(Tl) crystals with solid angle coverage about 90% of 4π . The energy resolution of the calorimeter for photons is $\sigma_E/E = 4.2\%/\sqrt{E(\text{GeV})}$, the angular resolution is about 1.5° . The directions of charged particles are measured by two coaxial cylindrical drift chambers covering 95% of 4π solid angle.

The analysis presented in this work is based on data recorded in 1997–1999 in two separate energy regions: 920–980 MeV and 1040–1380 MeV. Analysis of the ϕ -resonance region (980–1040 MeV) was published earlier [11]. In the first energy region the total integrated luminosity of 1.5 pb^{-1} was collected at 6 energy points. The region above the ϕ meson was scanned with a 10 MeV step. Total integrated luminosity accumulated in this region is about 9 pb^{-1} . The luminosity was measured with a systematic uncertainty of 3% using $e^+e^- \rightarrow e^+e^-$ and $e^+e^- \rightarrow \gamma\gamma$ reactions.

3 Event selection

For primary selection of

$$e^+e^- \rightarrow \omega\pi^0 \rightarrow \pi^0\pi^0\gamma \tag{1}$$

events the following criteria were applied:

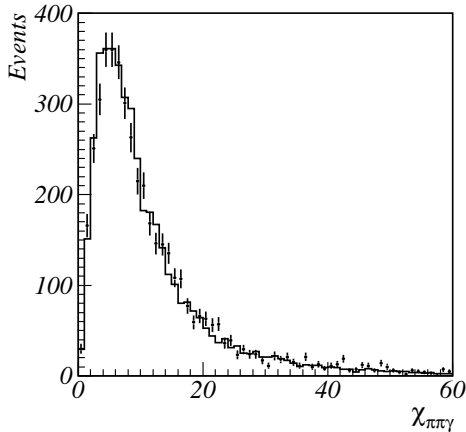


Figure 1: The $\chi_{\pi\pi\gamma}$ distribution for the experimental (points with error bars) and simulated (the histogram) events of the process (1).

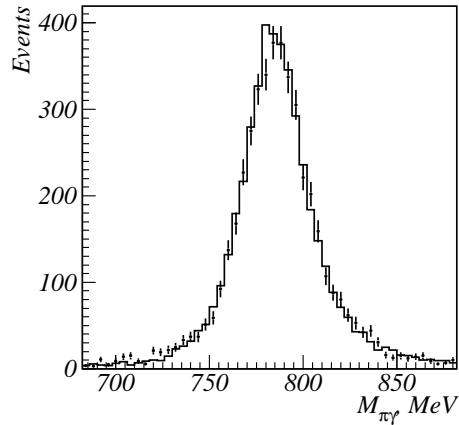


Figure 2: The $M_{\pi\gamma}$ distribution for the experimental (points with error bars) and simulated (the histogram) events of the process (1).

- five or more photons and no charged tracks are found in an event;
- the energy deposition in the calorimeter is more than $0.7E$;
- the total momentum of an event measured by the calorimeter is less than $0.15E$;

where E is a center of mass energy of e^+e^- pair. The main sources of background surviving these cuts are QED processes

$$e^+e^- \rightarrow 2\gamma, 3\gamma. \quad (2)$$

with extra photons either from the the beam background or splitting of electromagnetic showers in the calorimeter.

For each event satisfying primary selection criteria the kinematic fitting assuming $e^+e^- \rightarrow \pi^0\pi^0\gamma \rightarrow 5\gamma$ hypothesis was performed. As a result, two parameters: $\chi_{\pi\pi\gamma}$ — the χ^2 of the fit and $M_{\pi\gamma}$ — the π^0 recoil mass closest to that of ω meson were evaluated.

The $\chi_{\pi\pi\gamma}$ distribution for the events with $|M_{\pi\gamma} - 782| < 50$ and the π^0 recoil mass spectrum for the events with $\chi_{\pi\pi\gamma} < 30$ are plotted in figs.1 and 2. Good agreement between experimental distributions and simulation of the process (1) shows that there are no other significant contributions in the selected event sample. For final event selection the following cuts were applied:

$$\chi_{\pi\pi\gamma} < 30, |M_{\pi\gamma} - 782| < 50, \quad (3)$$

which reject the QED background (2) almost completely. In order to estimate residual background the experimental π^0 recoil mass spectrum was fitted by the sum of simulated spectrum of the process (1) and a linear background. As a result the estimated total number of background events did not exceed 1.5% of all selected events. This value was taken as a systematic error of the measured cross section of the process (1) related to the residual background.

Experimental data were collected in 40 energy points. In the energy region under study the cross section changes slowly so it was possible to reduce the number of energy points combining the neighboring ones. Resulting energies, their standard deviations, integrated luminosities (IL) and numbers of selected events (N) are listed in the Table 1. The detection efficiency for the process (1) was determined by simulation based on a formula from [12] which takes into account finite width of ω -meson. In the energy range from 1050 to 1400 MeV the efficiency was found to be constant and equal to 40%. Near the $e^+e^- \rightarrow \omega\pi^0$ threshold the number of events with the π^0 recoil mass below ω -meson mass increases sharply and the efficiency goes down. The energy dependence of the detection efficiency is presented in the Table 1.

4 Fitting of the cross section

The visible cross section $\sigma_{vis} = N/IL$ is related with the Born cross section of $e^+e^- \rightarrow \omega\pi^0 \rightarrow \pi^0\pi^0\gamma$ process as

$$\sigma_{vis}(E) = \varepsilon(E)\sigma_0(E)(1 + \delta(E)), \quad (4)$$

where $\delta(E)$ is a radiative correction calculated according to [13]. Radiative corrections for the different energies and obtained cross section values are listed in the Table 1. The cross section at $E = m_\phi$ was taken from [11]. Only statistical errors are shown in the table. The systematic error includes the error of the luminosity measurement (3%), the detection efficiency error (4%), possible background contribution (1.5%), and the error of radiative correction (1%). The total systematic error was estimated to be 5%.

Our results in comparison with the most precise CMD-2 [2], CLEO [4], and DM2 [8] measurements are shown in Fig.3. The cross sections from [2, 8] measured in the $\pi^+\pi^-\pi^0\pi^0$ channel were recalculated using the PDG value of $B(\omega \rightarrow \pi^0\gamma)$ [7]. The cross section from [4] was obtained from the $\tau \rightarrow \omega\pi\nu_\tau$ spectral function assuming the CVC hypothesis [14]. The CLEO results are in good agreement with ours while the CMD-2 measurements are about 10% lower, although the difference observed is smaller than the 15% systematic error quoted in [2]. There is a significant difference between the

Table 1: Energy, its standard deviation, integrated luminosity, detection efficiency, number of events, radiative correction and cross section of the process $e^+e^- \rightarrow \omega\pi^0 \rightarrow \pi^0\pi^0\gamma$

E , MeV	ΔE , MeV	IL , nb	ε	N	δ	σ_0 , nb
920	0.2	328	0.169	3	-0.148	0.06±0.04
940	0.2	289	0.312	15	-0.168	0.20±0.05
954	2.0	496	0.332	39	-0.157	0.28±0.05
973	4.3	373	0.352	68	-0.140	0.60±0.07
1020	–	–	–	–	–	0.74±0.02
1045	5.0	152	0.390	51	-0.100	0.96±0.13
1063	4.4	371	0.390	124	-0.093	0.95±0.09
1081	3.5	666	0.390	253	-0.086	1.07±0.07
1102	3.8	524	0.390	180	-0.080	0.96±0.07
1123	4.4	420	0.390	171	-0.074	1.13±0.09
1142	4.0	358	0.390	142	-0.070	1.09±0.09
1160	0.4	316	0.390	158	-0.066	1.37±0.11
1183	4.6	587	0.390	280	-0.061	1.30±0.08
1203	4.4	569	0.390	284	-0.057	1.36±0.08
1223	4.6	465	0.390	232	-0.054	1.35±0.09
1243	4.8	562	0.390	309	-0.050	1.48±0.08
1266	5.1	397	0.390	241	-0.046	1.63±0.11
1285	5.2	492	0.390	268	-0.043	1.46±0.09
1304	5.0	459	0.390	249	-0.040	1.45±0.09
1325	5.0	516	0.390	301	-0.038	1.55±0.04
1344	5.8	676	0.390	387	-0.036	1.52±0.08
1363	4.6	857	0.390	497	-0.034	1.54±0.07
1380	0.5	470	0.390	234	-0.033	1.32±0.09

results of DM2 [8] and CLEO [4]. For the cross section fitting we used our data together with the data from CLEO.

The energy dependence of the process (1) cross section was written as a sum of contributions from $\rho(770)$ and its excitations ρ' and ρ'' :

$$\sigma_0(E) = \frac{4\pi\alpha^2}{E^3} \left(\frac{g_{\rho\omega\pi}}{f_\rho} \right)^2 \left| \frac{m_\rho^2}{D_\rho} C_{\rho\omega\pi} + A_1 \frac{m_{\rho'}^2}{D_{\rho'}} C_{\rho'\omega\pi} + A_2 \frac{m_{\rho''}^2}{D_{\rho''}} C_{\rho''\omega\pi} \right|^2 P_f(E). \quad (5)$$

Here α is a fine structure constant and $g_{\rho\omega\pi}$ is a $\rho \rightarrow \omega\pi$ coupling constant. The f_ρ coupling constant was calculated from the $\rho \rightarrow e^+e^-$ decay width: $\Gamma_{\rho ee} = 4\pi m_\rho \alpha^2 / 3 f_\rho^2$. The expression m_ρ^2 / D_ρ represents ρ -meson Breit-Wigner amplitude with $D_\rho = m_\rho^2 - E^2 - iE\Gamma_\rho(E)$, where m_ρ and $\Gamma_\rho(E)$ denote the ρ meson mass and energy-dependent total width respectively. The real

parameters $A_i = g_{\rho_i\omega\pi}/g_{\rho\omega\pi} \cdot f_\rho/f_{\rho_i}$ are the ratios of the coupling constants of different ρ states. The factor $P_f(E)$ describes the energy dependence of the final state phase space. In the case of infinitely narrow ω resonance $P_f(E) = 1/3 \cdot q_\omega^3 B(\omega \rightarrow \pi^0\gamma)$, where q_ω is an ω -meson momentum. This approximation is good for the energy range above 1050 MeV, but at energies close to the $e^+e^- \rightarrow \omega\pi^0$ threshold it is more adequate to use precise formula taking into account finite width of the ω meson [12]. The Blatt-Weisskopf factors $C_{\rho_i\omega\pi}$ restricting fast growth of the partial widths, were taken in the form [6]:

$$C_{\rho\omega\pi} = \frac{1}{1 + (Rq_\omega(E))^2}, \quad C_{\rho_i\omega\pi} = \frac{1 + (Rq_\omega(m_{\rho_i}))^2}{1 + (Rq_\omega(E))^2}, \quad i = \rho', \rho'', \quad (6)$$

The range parameter R was assumed to be the same for ρ , ρ' and ρ'' mesons. The energy dependence of the $\rho(770)$ total width was expressed as:

$$\Gamma_\rho(E) = \Gamma_\rho(m_\rho) \left(\frac{m_\rho}{E}\right)^2 \left(\frac{q_\pi(E)}{q_\pi(m_\rho)}\right)^3 C_{\rho\pi\pi}^2 + \frac{g_{\rho\omega\pi}^2}{12\pi} q_\omega^3(E) C_{\rho\omega\pi}^2, \quad (7)$$

where q_π is the pion momentum, $C_{\rho\pi\pi}$ is the Blatt-Weisskopf factor for $\rho \rightarrow \pi^+\pi^-$ decay [15]:

$$C_{\rho\pi\pi}(E) = \sqrt{\frac{1 + (Rq_\pi(m_\rho))^2}{1 + (Rq_\pi(E))^2}}. \quad (8)$$

There is no generally accepted description of the shapes of the broad excited states ρ' and ρ'' . In [6] constant total width were assumed, while in [16] the total widths varied with energy as a sum of the partial widths of all main decay modes. We considered the both approaches in order to understand model dependence of the fit parameters.

The fit results obtained for three classes of models are listed in the Table 2. The fit parameters are sensitive to the variation of the range parameters R in the Blatt-Weisskopf factors. In the Table 2 we show the intervals of the fit parameter variation when R ranges from 0 to 2 GeV⁻¹. The typical errors of the parameters obtained for each specific model are listed in the fourth column of the Table 2.

In the model 1 the constant widths of ρ' and ρ'' were assumed. The mass and width of the ρ'' meson were fixed to their PDG values [7]: $m_{\rho''} = 1700$ MeV, $\Gamma_{\rho''} = 235$ MeV. The obtained value of the ρ'' amplitude A_2 is compatible with zero, so the final fit result for the model 1 is given for A_2 fixed to zero. Let us discuss the choice of an upper boundary for the R parameter. Small values $g_{\rho\omega\pi} < 13$ GeV⁻¹ found for $R > 2$ GeV⁻¹ are in conflict with the QCD sum rules estimation 16 GeV⁻¹ [17] and experimental

Table 2: The fit results for various models described in the text.

	Model 1	Model 2	Model 3	Error
$R, \text{ GeV}^{-1}$	0–2	0–2	0–2	
$g_{\rho\omega\pi}, \text{ GeV}^{-1}$	16.1–13.3	15.6–13.2	15.6–12.9	0.3–0.4
$m_{\rho'}, \text{ MeV}$	1460–1520	–	$\equiv 1400.$	10
$\Gamma_{\rho'}, \text{ MeV}$	380–500	–	$\equiv 500.$	20–30
A_1	-(0.22–0.24)	$\equiv 0.$	-(0.04–0.08)	0.01–0.02
$m_{\rho''}, \text{ MeV}$	–	1710–1580	1620–1550	15–20
$\Gamma_{\rho''}, \text{ MeV}$	–	1040–490	580–350	70–20
A_2	$\equiv 0.$	-(0.22–0.20)	-(0.18–0.13)	0.1
χ^2/ND	(52–48)/35	(47–48)/35	(43–44)/34	

value of 14.4 GeV^{-1} , obtained from the $\omega \rightarrow 3\pi$ decay width assuming that $\omega \rightarrow \rho\pi$ mechanism dominates in this decay. Only for $R \sim 0$ the extracted mass and width of the ρ' meson are compatible with their PDG values[7]. However in this case the fit yields the lowest confidence level of $P(\chi^2) = 3\%$.

Models 2 and 3 take into account energy dependence of the total widths of ρ' and ρ'' mesons. Since branching ratios of ρ' and ρ'' decays are practically unknown [7] the energy dependence of the sum of all rapidly growing partial widths of their multihadron decays was approximated as the energy dependence of $\rho_i \rightarrow \omega\pi$ width:

$$\begin{aligned}
 \Gamma_{\rho_i}(E) &= \Gamma_{\rho_i}(m_{\rho_i}) \left[(1 - B_{\rho_i \rightarrow \pi\pi}) \left(\frac{q_\omega(E)}{q_\omega(m_{\rho_i})} \right)^3 C_{\rho_i\omega\pi}^2 \right. \\
 &\quad \left. + B_{\rho_i \rightarrow \pi\pi} \left(\frac{m_{\rho_i}}{E} \right)^2 \left(\frac{q_\pi(E)}{q_\pi(m_{\rho_i})} \right)^3 C_{\rho_i\pi\pi}^2 \right], \quad (9)
 \end{aligned}$$

For the $\rho'' \rightarrow 2\pi$ branching fraction we use the theoretical estimation: $B_{\rho'' \rightarrow \pi\pi} = 10\%$ [18]. For the ρ' meson the value $B_{\rho' \rightarrow \pi\pi} = 50\%$ was chosen which, we think, reflects experimental situation more correctly than the theoretical prediction 25% [18]. The only difference between the models 1 and 2 which both consider only one excited ρ state is that the model 2 assumes its total width energy dependent. But the fit results for these two models are quite different. Particularly the mass found for the model 2 is close to the PDG value of the ρ'' -meson mass. On the other hand there is a definite signal of the ρ' meson with a mass of 1320–1400 MeV and 400–500 MeV width in the pion form factor data [3, 5]. Therefore we also considered the model 3 with two excited ρ states, in which the mass and width of the ρ' meson were fixed

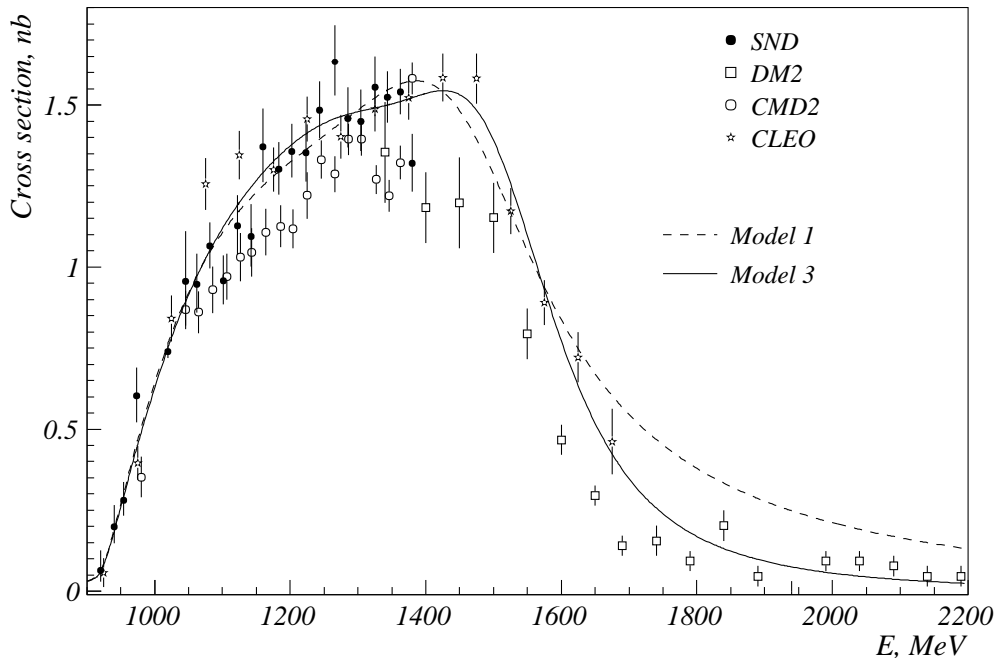


Figure 3: The cross section of the reaction $e^+e^- \rightarrow \omega\pi^0 \rightarrow \pi^0\pi^0\gamma$. The results of the SND (this work), DM2 [8], CMD [2], CLEO [4] experiments are shown. Curves are results of fitting to the data in model 1 and 3 with $R = 0$.

to $m_{\rho'} = 1400$ MeV and $\Gamma_{\rho'} = 500$ MeV. This model yields the best fit to the experimental data: $P(\chi^2) \approx 13\%$. Fitting curves corresponding to the models 1 and 3 with $R = 0$ are shown in figure 3.

The main conclusions from the analysis of the fit results are the following. Fitting of the same experimental data by models with fixed and energy-dependent total widths of the excited states yields quite different parameters of these states. This is caused by strong energy dependence of the phase space for the main decay modes of ρ' and ρ'' mesons and this effect should be taken into account in the fitting of experimental data. Satisfactory description of the experimental cross section was obtained in the model with two excited states with the masses $m_{\rho'} = 1400$ MeV and $m_{\rho''} \approx 1600$ MeV in which contribution of the higher state dominates. However this result contradicts the theoretical expectation [18, 19], where ρ' and ρ'' are considered as $2S$ and $1D$ $q\bar{q}$ states respectively and the larger contribution of the lower $2S$ excitation was predicted. Thus, with the new experimental data the situation in the isovector sector remains unclear. The main problem for data analysis is the absence of consistent phenomenological description of the shapes of broad resonances with strong energy dependence of partial widths.

5 Summary

In this work the cross section of the $e^+e^- \rightarrow \omega\pi^0 \rightarrow \pi^0\pi^0\gamma$ reaction was measured from the threshold up to 1.4 GeV with a 5% systematic accuracy. This is the most precise measurement of the $e^+e^- \rightarrow \omega\pi^0$ cross section in this energy range. Our data are in a good agreement with the CLEO measurement of $\tau \rightarrow \omega\pi\nu_\tau$ spectral function [4]. The combined fit to our and CLEO data was performed in the vector meson dominance model taking into account the contributions of ρ , ρ' and ρ'' states. The experimental data can be reasonably well approximated assuming existence of only one excited state but its mass is strongly model-dependent and varies from 1460 to 1700 MeV for different descriptions of the resonance shape. The best fit to the data was obtained for the model with two excited states in which the higher state with $m_{\rho''} \approx 1600$ MeV dominates.

This work is supported in part by the Russian Fund for Basic Researches (grants No. 99-02-16815, 99-02-17155) and STP “Integration” (grant No. 274).

References

- [1] M.N.Achasov et al., Phys. Lett. B 462 365 (1999).
- [2] R.R. Akhmetshin et al., Phys.Lett. B 466 392 (1999).
- [3] S. Anderson et al., e-print hep-ex/9910046.
- [4] K.W. Edwards et al., Phys. Rev. D 61 (2000), e-print hep-ex/9908024.
- [5] R. Barate et al., Z.Phys. C 76 15 (1997).
- [6] A.B. Clegg, A. Donnachie, Z.Phys. C62 455 (1992).
- [7] Review of Particles Physics, The Eur. Phys. J. C 3, (1998).
- [8] D. Bisello et al., Preprint LAL-90-71, Nucl. Phys. Proc. Suppl. 21 111 (1991).
- [9] S.I. Dolinsky et al., Phys.Lett. B174, 453 (1986).
- [10] M.N. Achasov et al., e-print hep-ex/9909015. To be published in Nucl. Instr. Meth.
- [11] M.N. Achasov et al. To be published in JETP.

- [12] M.N. Achasov et al., Nucl. Phys. B 569 158 (2000).
- [13] E.A. Kuraev, V.S. Fadin, Sov. J. Nucl. Phys. 41 (1985) 466.
- [14] Y.S. Tsai, Phys. Rev. D 4 2821 (1971).
- [15] J. Pisut and M. Roos, Nucl. Phys. B 6, 325 (1968).
- [16] N.N. Achasov, A.A. Kozhevnikov, Phys.Rev. D55 2663 (1997).
- [17] M. Lublinsky. Phys. Rev. D 55, 249 (1996).
- [18] T. Barnes et al., Phys.Lett. B385 391 (1996).
- [19] S. Godfrey, N. Isgur, Phys. Rev. D 32 189 (1985).